CHAPTER 5

The role of π-linkers and electron acceptors in tuning the nonlinear optical properties of BODIPY based zwitterionic molecules

Abstract

Intramolecular charge transfer process can play a key role to develop strong nonlinear optical (NLO) response in a molecule for technological application. Herein, two series of boron dipyromethane (BODIPY) based push-pull systems have been designed with zwitterionic donor-acceptor groups and their NLO properties have been evaluated using density functional theory based approach. Different π-conjugated linkers and electron acceptor groups are taken to understand their role in tuning the NLO properties. The molecules are analyzed through HOMO-LUMO gap, frontier molecular orbitals, polarizability, hyperpolarizability, Δr index, transition dipole moment density, ionization potential, electron affinity and reorganization energy for hole and electron. It is found that with the introduction of different π-linkers in the molecule, planarity is maintained and HOMO-LUMO gap is systematically decreased which leads to large NLO response. It is noted that the electronic absorption wavelength maxima found in the near-infrared region. The results show that compared to pyridinium acceptor group, imidazolium acceptor group in the BODIPY systems amplifies NLO response to a larger extent. It is also observed that BODIPY based dye having imidazolium acceptor and thienothiophene π-linker shows the highest first hyperpolarizability value. Furthermore, the charge transfer occurs in the z-direction as the z-component of the first hyperpolarizability is the dominant factor in this system. Here the designed molecules show characteristics reorganization energy value which is a deciding factor for rate of hole/electron transport property for favorable intermolecular coupling. As a whole, this theoretical work highlights that π-conjugated linkers and electron acceptor groups can be used judiciously to design new molecular systems for optoelectronic application.

5.1. Introduction

Materials with high nonlinear optical (NLO) properties have gained much attention in recent years, as they offer potential application in optoelectronic and photonic devices in regulation of optical switching, micro fabrication and imaging, telecommunication, laser technology, data storage etc.[1-9] Different types of materials of both inorganic[10] and organic[11-13] origin have been investigated for their interesting nonlinear optical properties. However among them, organic materials with high NLO response are proven to be the optimum choice due to their tunability.[7, 14] Most of the organic NLO materials are push-pull molecules having π-conjugated system linking an electron donor (D) to an electron acceptor (A) group.[15] The NLO properties in these compounds are developed due to high polarization of π electrons along the conjugated backbone. The first hyperpolarizability (β) is associated with the intramolecular charge transfer (ICT) from donor group to electron acceptor group. Several studies confirmed that by optimizing the donor and acceptor groups, π-linker and ring twisting in the push-pull system, the ICT process can be amplified and hence the NLO response.[16-18] The main strategies for designing efficient NLO material are based on the choice of suitable donor and acceptor groups and π conjugated bridge.[19, 20] Albert et al. suggested an approach that by introducing zwitterionic behaviour in a conjugated molecule one can enhance the NLO property by providing low energy charge transfer.[21, 22] Some researchers also revealed that zwitterionic D and A groups positioned at opposite end of conjugated system of the chromophores can ameliorate the NLO response.[12, 23] Xiong et al. synthesized thermally stable zwitterionic picolinium(dicyano) esterquinodimethane chromophore having β value of 1800×10^{-30} esu.[24] All these facts prompt us to design and investigate zwitterionic systems crafted by different donors and acceptors with high NLO response.

Boron dipyromethane (BODIPY) based push-pull chromophore is an area of recent interest which has been taken for the present investigation. BODIPY dyes are well known for their desirable photophysical properties as they posses strong absorption band in UV-Vis region, high fluorescence quantum yield,[25, 26] two photon absorption properties etc.[27] BODIPY dyes are widely used in photodynamic therapy,[28] as chemosensor,[29]

fluorosensor[30] etc. Extensive researches have been done on the molecular structure and optical property of BODIPY dye but very few have reported about the BODIPY based push-pull zwitterionic systems. In this work the main strategy is introduction of donor and acceptor groups to the opposite ends of BODIPY core at 2, 6 positions. Imidazolium compounds are known for significant absorption in the entire UV region and for its fluorescence property.[31, 32] It is reported that imidazolium cation provides remarkable contribution to enhance NLO response.[33, 34] To investigate the effect of different electron acceptors and π-conjugated linkers on the NLO property of BODIPY system, 10 new BODIPY based D-π-A dyes are designed (Fig. 5.1). Pyridinium and imidazolium ions are taken for positively charged acceptor group and phenoxide group is taken for negatively charged donor group. Four π-spacers such as ethylene, cis-thiophene with respect to BODIPY, trans-thiophene with respect to BODIPY and thienothiophene are used as 1st and 3rd π-linker and BODIPY is used as 2nd π-linker.

This paper deals primarily with the theoretical calculation of optoelectronic properties of newly designed molecules using density functional theory (DFT) based methods. We focus our work to find the influence of different π-conjugated linkers and π-acceptors on the NLO properties of molecules. DFT and TDDFT calculations have been carried out to evaluate the molecular properties including frontier molecular orbitals, absorption spectra, polarizability and hyperpolarizability, ionization potential (IP), electron affinity (EA) and reorganization energy of hole and electron. It is exhibited that with increasing π-electron delocalization and substitution of pyridinium cation by imidazolium cation in the BODIPY based systems, NLO response is amplified. The present work will provide a direction to the researchers for the synthesis of novel NLO materials of BODIPY based dyes for technological application.

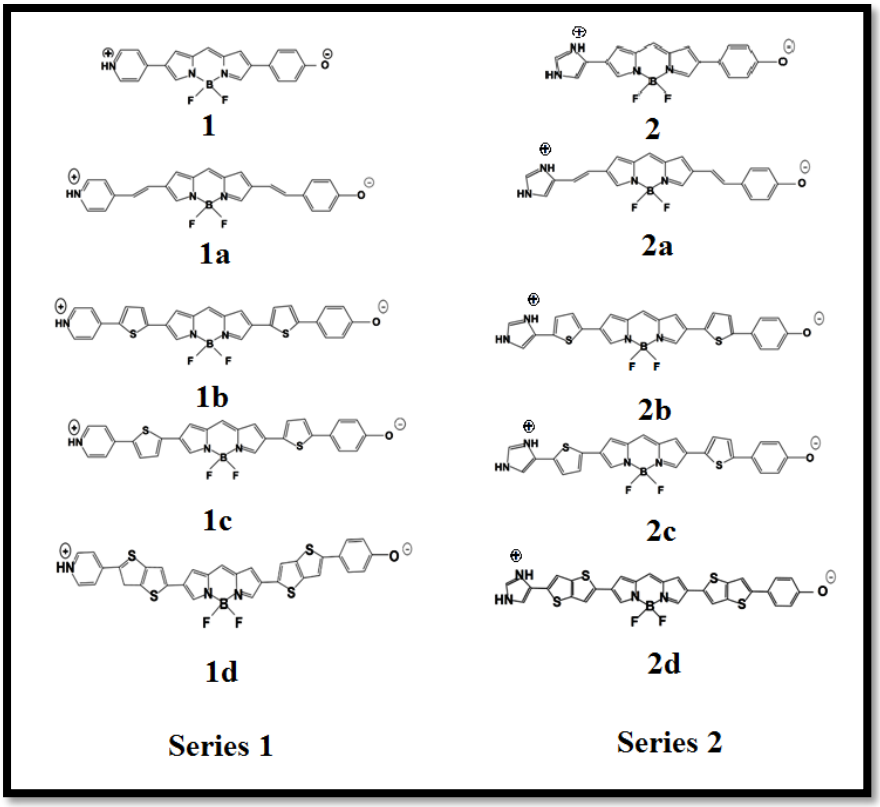

Fig. 5.1. Chemical structures of the BODIPY-based dyes under investigation.

5.2. Theoretical Background and Computational Details

Geometry optimization of the designed molecules are performed in the gas phase using Gaussian 09 program at B3LYP/6-311++G(d,p) level of theory.[35] The molecules are optimized at minimum energy level and no imaginary frequency is found which signifies the stationary point of minima. All the restricted B3LYP solutions obtained are stable. Prakasam et al. investigated second order hyperpolarizability and absorption property of triphenylamine based organic sensitizers with the B3LYP/6-311++G(d,p) method.[36] Very recently Avramopoulos and co-workers designed photochromic material with switchable nonlinear optical properties by employing density functional method with CAM-B3LYP functional.[37] DFT based B3LYP and CAM-B3LYP are good functionals for explanation of the NLO behaviour of the studied system. Hence, in order to analyze the NLO behaviour of the designed D-π-A system, dipole moment (μ_{total}), average polarizability (α) and first hyperpolarizability (β) are evaluated using B3LYP functional as well as with CAM-B3LYP[38] functional with 6-311++G(d,p) basis set to

include long range correction for improving the charge transfer characteristics in the Gaussian 09 software.[39]

Dipole moment was calculated using the following equations,

$$\mu_{tot} = \sqrt{\mu_x^2 + \mu_y^2 + \mu_z^2} \qquad (5.1)$$

where, μ_x, μ_y, and μ_z are components of the dipole moments in the x, y, and z directions, respectively.

Average polarizability ($< \alpha >$) was calculated using the following equation [40]

$$< \alpha > = \frac{1}{3} (\alpha_{xx} + \alpha_{yy} + \alpha_{zz}) \qquad (5.2)$$

α_{xx}, α_{yy} and α_{zz} are the polarizability tensor components.

The first hyperpolarizability (β_{total}) can be expressed as [40]

$$\beta_{total} = (\beta_x^2 + \beta_y^2 + \beta_z^2)^{\frac{1}{2}} = [(\beta_{xxx} + \beta_{xyy} + \beta_{zzx})^2 + (\beta_{yyy} + \beta_{yzz} + \beta_{yxx})^2 + (\beta_{zzz} + \beta_{zxx} + \beta_{zyy})^2]^{1/2} \qquad (5.3)$$

β_{xxx}, β_{xyy}, β_{zzx}, β_{yyy}, β_{yzz}, β_{yxx}, β_{zzz}, β_{zxx} and β_{yyy} are hyperpolarizability tensors along x, y and z direction respectively.

The transition dipole moment (TDM) density has been evaluated on the basis of dipole moment integral between the occupied and virtual molecular orbitals. The TDM density can be calculated and visualized using the Multiwfn wave function analyzer.[41] The charge transfer length during electron excitation in D-π-A system is defined as Δr index. This is defined by the following equation [42]

$$\Delta r = \frac{\sum_{i,l}(K_i^l)^2 |\langle \varphi_l | r | \varphi_l \rangle - \langle \varphi_i | r | \varphi_i \rangle|}{\sum_{i,l}(k_i^l)^2} \qquad (5.4)$$

where i and l indices run over all occupied and vertical MOs, Φ is orbital wave function,

$$K_i^l = X_i^l + Y_i^l \qquad (5.5)$$

X_i^l and Y_i^l denotes the configuration coefficient corresponding to $i \rightarrow l$ excitation and $l \rightarrow i$ de-excitation. The Δr index is calculated using Multiwfn software.

Ionization Potential (IP) defines the energy changes due to removing of electrons or adding holes from/to the neutral molecule. On the other hand, electron affinity (EA) quantifies the energy changes for adding electrons or removing holes in the same. This can be expressed as:[43]

$$\boldsymbol{IP = E_{Cation} - E_{Neutral}} \quad \text{and} \quad \boldsymbol{EA = E_{Neutral} - E_{Anion}} \quad (5.6)$$

E denotes energy of the respective systems. Hole transport reorganization energy (λ_{hole}) and electron transport reorganization energy ($\lambda_{electron}$) are calculated as:[44]

$$\boldsymbol{\lambda_{hole} = \lambda_1 + \lambda_2 = (E_0^+ - E_+) + (E_+^0 - E_0)} \quad (5.7)$$

$$\boldsymbol{\lambda_{electron} = \lambda_3 + \lambda_4 = (E_0^- - E_-) + (E_-^0 - E_0)} \quad (5.8)$$

Here, E_0, E_+ and E_- represent the energy of neutral, cation and anion species respectively in their optimized geometries. $E_0^{+/-}$ and $E_{+/-}^0$ represent energy of cation/anion with the optimized structure of neutral species and energy of neutral species with the optimized structure of cation /anion geometry.

5.3. Results and Discussions

5.3.1. Electronic structure

Electronic structure of molecules play a key role in regulating nonlinear optical properties as it depends on the geometry of the molecular systems. Here Fig. 5.1 represents BODIPY molecules with different π-linkers and acceptors with phenoxide donor. The optimized structures of the molecules, dihedral angles and bond angles are given in electronic supplementary information (Fig. S1-S10 and Table S1-S10). For smooth electron transfer process from donor unit to acceptor unit, dye must have co-planarity between the donor unit-bridging unit-acceptor unit (D-π-A).[45] It is found that most of the dyes maintain co-planarity as the dihedral angles are close to 0^o and 180^o and bond angles are close to 120^o. It is also to be noted that dye 2d has perfect planar geometry as the geometrical parameters are very close to ideal. Thus we can say that inclusion of different π-linkers favour planarity in the investigated systems. It is reported that attaching an unsubstituted phenyl ring to the BODIPY core, fluorescence quantum yield (φ_f) decreases compared to BODIPY alone. Whereas, incorporation of two methyl

groups in the BODIPY system restricts the motion of phenyl ring and increases φ_f of the molecule.[46] So we can expect incorporation of proper π-linkers should increase the NLO response.

The charge transfer process is highly dependent on the energy difference between HOMO and LUMO (Δ*E*). The frontier molecular orbital (FMO) theory helps to predict the chemical stability of the molecule.[47, 48] Usually LUMO defines the capacity of acceptance of electron and HOMO classifies electron donating ability.[49] Low Δ*E* value indicates chemically soft molecule whereas high Δ*E* value signifies chemically hard molecule. Polarizability can be enhanced with the increase of the softness in a molecule which facilitates the NLO response.

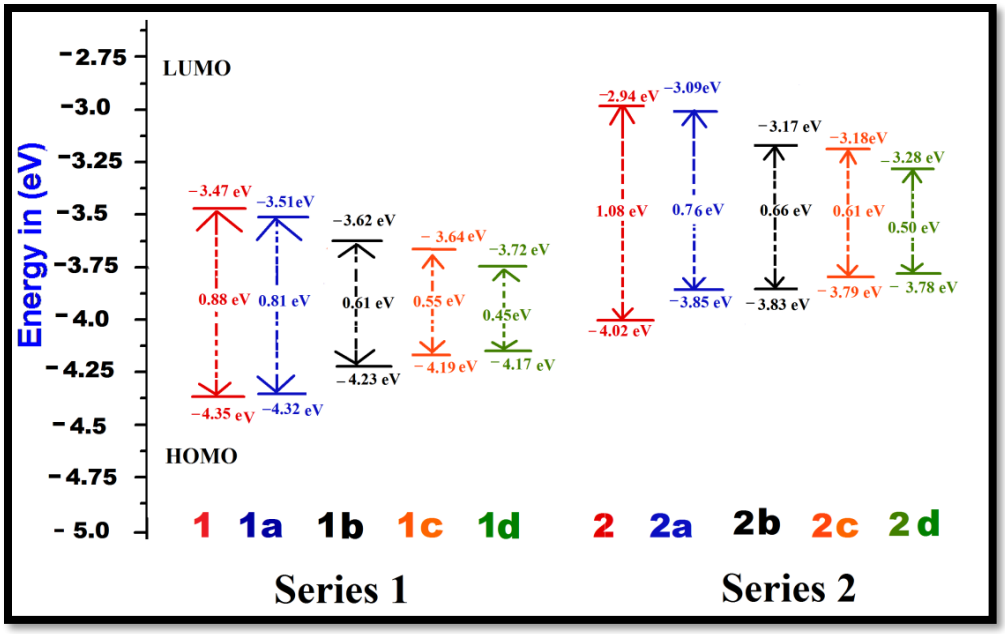

Fig. 5.2. Energy level diagrams of the dyes in gas phase at B3LYP/6-311++G (d,p) level of theory.

The FMO energy levels along with the HOMO-LUMO gaps are represented in Fig. 5.2. Proper inclusion of acceptor and donor units at 2 and 6 positions of BODIPY make the molecule zwitterionic and the HOMO-LUMO energy gap is found to reduce. Now, the compounds which are studied can be categorized into two sets such as BODIPY based pyridinium acceptor (Series 1) and imidazolium acceptor (Series 2). Upon introduction of different π-linkers in BODIPY framework in series 1 and 2, Δ*E* starts

diminishing from the values 0.88 eV and 1.08 eV in a very systematic way. Upon insertion of −CH=CH− (1a and 2a), cis-thiophene (1b and 2b) and trans thiophene (1c and 2c) groups in the BODIPY system, Δ*E* reduces successively. However, when thioenothiophene groups are inserted (dye 1d and 2d), least Δ*E* of 0.45 eV and 0.50 eV are found. This clearly reveals that thioenothiophene π-linkers reduce the HOMO-LUMO gap more in the imidazolium system compared to pyridinium acceptor system. It is expected that by maintaining planarity, extended conjugation and low Δ*E* gap, molecules should achieve high NLO response. In many cases differences in the energy difference between HOMO-LUMO of the designed dyes are very small. It may be due to the limitation of the method used. Zhang et al. synthesized and performed DFT based B3LYP calculation on a series of highly polarizable bis(N,N-diethyl) aniline based chromophore. Where the differences of reported energy differences of the compounds are also very low.[50] So, these values can be taken for explanation of the NLO behaviour of the investigated compound. The order of HOMO-LUMO energy gap of series 1 and 2 are 1d < 1c < 1b < 1a < 1 and 2d < 2c < 2b < 2a < 2. Therefore it can be predicted that all these molecules will show higher absorption wavelength and would be excellent candidate for NLO material for various photoelectronic application. The modification of π-conjugated linker by tailoring the structure would be a strategy to obtain high NLO activity. In order to understand the distribution pattern of HOMO and LUMO, we analyze frontier molecular orbitals of the investigated dyes which are given in Fig. 5.3. From FMO diagram it is evident that for Series 1, HOMO and LUMO of all the chromophores are delocalized throughout the molecule. Whereas for Series 2, the HOMO is localized on the phenoxide donor part and π-conjugated part; and LUMO is localized mainly on the imidazolium acceptor part of the molecule. This fact signifies the electron donating ability of phenoxide ion and electron acceptance nature of imidazolium cation. Overall, the calculated geometrical parameters indicate that planarity and delocalization in a molecule can be adjusted by varying the π-linkers which are significant characteristics for tuning optoelectronic properties.

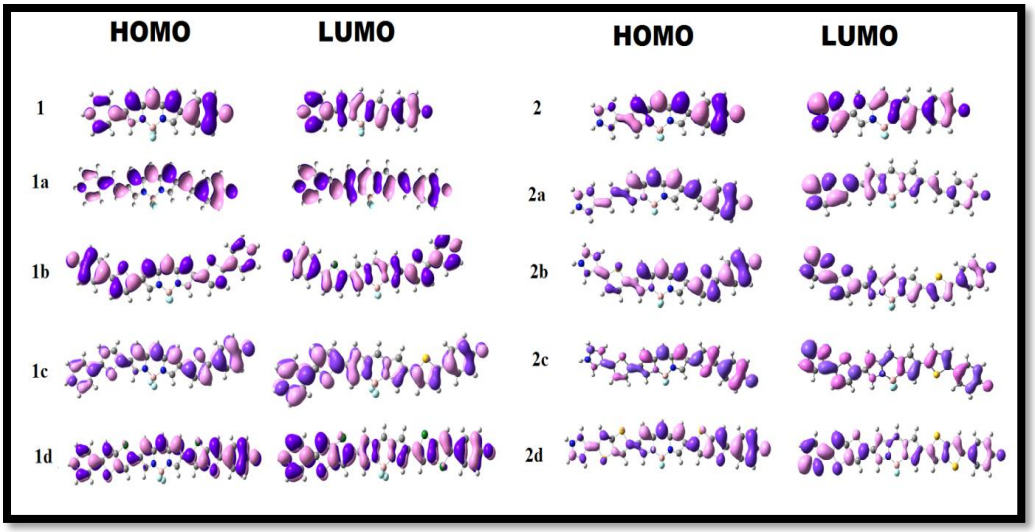

Fig. 5.3. Frontier molecular orbitals of the dyes in the gas phase at B3LYP/6-311++G (d,p) level of theory.

5.3.2. NLO properties

For the evaluation of NLO properties of the dyes the magnitude of static dipole moment, linear response (polarizability) and nonlinear response (1st hyperpolarizability) need to be assessed. Benchmarking of the computational model for the NLO calculation has been done with some well known push–pull systems given in electronic supplementary information[51] (Table S14). Comparison between theoretically calculated results and experimental results of hyperpolarizability show good agreement. Benchmarking exercise demonstrates that hyperpolarizability value for B3LYP functional is closer to experimental value compared to CAM-B3LYP functional. Here our main objective is to find the effect of zwitterionic donor-acceptor group and π-linkers on the hyperpolarizability value. So for the explanation of changes of hyperpolarizability values with the structural modification in the framework of donor-acceptor molecule in the gas phase we keep other tuning parameters unchanged. Hence to find out the influence of π-conjugated linkers and electron acceptor groups on NLO properties of Series 1 and Series 2 compounds, these parameters are calculated with B3LYP and range-separated CAM-B3LYP functionals with a standard basis set, 6–311++G(d,p) and the results are tabulated in Table 5.1 and Table S12 (Electronic supplementary information). In the following discussion results have been illustrated using B3LYP functional. The average

polarizability ($\Delta\alpha$) of the dyes increases in the following order a < b < c < d for both the series and the results found using B3LYP and CAM-B3LYP functionals follow the same trend. Looking at Table 5.1 one can find the average polarizability of dye 1 and 2 are 103.37 $\times 10^{-24}$ esu and 83.72 $\times 10^{-24}$ esu respectively. With the addition of ethylene π-linkers as 1st and 3rd conjugator in 1 and 2 dye, $\Delta\alpha$ increases by 61 $\times 10^{-24}$ esu and 65 $\times 10^{-24}$ esu respectively. The polarizability further increases with the addition of thiophene π-linker at cis and trans position of BODIPY. It is found that average polarizability reaches at maxima and values increased by 242 $\times 10^{-24}$ esu and 238$\times 10^{-24}$ esu when thioenothiophene groups are incorporated in the parent compounds (Table 5.1). Therefore, Table 5.1 and Table S12 indicate that with the modification by different π-conjugated linkers, polarizability enhances systematically. The highest polarizability is found for dye 1d of 345.52 $\times 10^{-24}$ esu with smallest ΔE (Table 5.1). It is known that small energy gap between HOMO and LUMO influence the polarizability of the molecule and the results are in accordance with the calculated HOMO-LUMO gap.

Table 5.1. Dipole moment (μ), static polarizability ($\Delta\alpha$) and $\mu\beta$ of the studied dyes at the B3LYP/6-311++G(d,p) level of theory.

Molecules	μ **Debye**	$\Delta\alpha$ 10^{-24} **esu**	$\mu\beta$ 10^{-48} **esu**
1	27.24	103.37	9359
1a	31.50	163.64	19561
1b	34.19	230.47	23968
1c	35.34	234.66	26900
1d	41.22	345.52	36058
2	33.63	83.72	30308
2a	42.40	147.55	80177
2b	46.53	208.24	102970
2c	48.16	211.91	107734
2d	57.28	320.46	182951

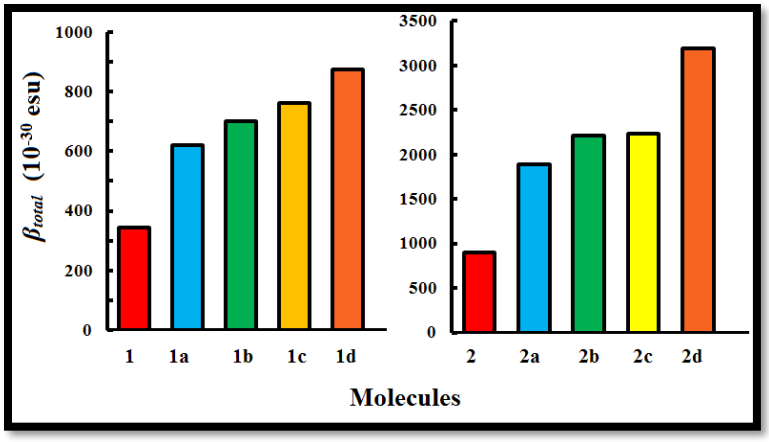

Fig. 5.4. First hyperpolarizability of BODIPY based dyes studied at B3LYP/6-311++G (d,p) level of theory.

First hyperpolarizability is connected with the ICT process. This is due to the flow of electron density from D to A via π-conjugated bridge, which is discussed in more details latter. Among the investigated molecules, dipole moment has been found highest for dye 2d while lowest value is found for dye 1. It is reported that large dipole moment and hyperpolarizability play significant role for poled polymer.[52] So, high dipole moment of these molecules is likely to enhance the NLO response. First hyperpolarizability is graphically represented in Fig. 5.4. Calculation of β_{total} value using B3LYP and CAM-B3LYP functionals follow the same trend of increasing order. An increase in β_{total} value of 557 $\times 10^{-30}$ esu is observed in case of imidazolium acceptor group (dye 2) compared to pyridinium acceptor (dye 1), which proves better electron acceptance power of imidazolium cation.[34] This is also found in the frontier molecular orbital. Changes in the π-conjugation length due to inclusion of 1st and 3rd π-linkers affect NLO property of the studied systems. For Series 1 and Series 2 with the incorporation of ethylene π-linker, β_{total} values are almost doubled. It is found that with the addition of thio-linkers in both series 1st hyperpolarizability increases systematically. Compared to cis-thiophene π-linkers, trans-thiophene π-linkers improve β_{total} value by 60 $\times 10^{-30}$ esu in dye 1c and 24 $\times 10^{-30}$ esu in dye 2c. When thienothiophene molecules are added to dye 1 and 2, β_{total} value increases by 531 $\times 10^{-30}$ esu and 2293 $\times 10^{-30}$ esu respectively. This can be correlated with the HOMO-LUMO gap of the molecule as shown in Fig 5.2. It is known that 1st order hyperpolarizability increases with the decrease of ΔE.[53, 54] If we compare

Fig. 5.2, Fig. 5.4 and Table 5.1, it can be found that for all cases ΔE gap is inversely proportional to the dipole moment, linear polarizability and 1st order hyperpolarizability. The β_{total} values of the two series decreases in the following order 1d > 1c >1b >1a > 1 and 2d > 2c > 2b > 2a >2 for B3LYP as well as CAM-B3LYP functional. It is observed that BODIPY based dyes having imidazolium acceptor and thienothiophene π-linker in dye 2d shows the highest β_{total} and $\mu\beta$ value of 3194×10^{-30} esu and 18.29×10^{-44} esu respectively. This NLO response can be attributed to the effective charge transfer from D to A moiety. The computed β_{total} value of 2d is 4110 times higher than the 1st hyperpolarizability value of urea, which is used as the reference in organic systems. It is also to be noted that in both series, the order of β_{total} value is in conformity with the average polarizability. For a better insight, we have reported the components of 1st hyperpolarizability in Table 5.2 and Table S13 (Electronic supplementary information). Yu et al. argued that β_y controls the β_{total} of 2,3-naptho-15-crown-5 ether for some metal cation complexes.[55] They conclude that during the polarization process the charge flows in the y direction. Results in Table 5.2 and Table S13 indicate that for the investigated systems β_{total} is dominated by β_z component. The contribution of β_x is negligible. Therefore, we can surmise that during the polarization process maximum charge is expected to transfer along the z direction.[56]

Table 5.2. β_x, β_y, and β_z components (10^{-30} esu) of studied molecules (1 to 2d) obtained from DFT calculation (B3LYP functional), employing the 6-311++G(d,p) basis set.

Molecules	β_x	β_y	β_z
1	-9.84	83.69	333.09
1a	11.0	146.99	603.38
1b	-4.45	83.37	696.03
1c	-0.296	72.43	757.71
1d	-12.7	155.17	860.81
2	-6.39	102.47	895.35
2a	15.4	-243.53	1875.16
2b	6.38	70.57	2212.42
2c	48.2	-309.23	2215.48
2d	-16.4	-417.39	3166.54

To explain the origin and variation of NLO response major transition energy, Δ*r* index, integral overlap of hole electron distribution (*s*) and distance between centroid of hole and electron (*D*) are tabulated (Table 5.3). From Table 5.3 we can find that, for all the cases Δ*r* indices is larger than 2.0 hence they may be regarded as charge transfer (CT) mode.[42] If we compare Fig. 5.4 and Table 5.3, we can find that both β_{total} and Δ*r* indices increase with the π-conjugated linkers showing same trend of increment. 2d compound shows highest Δ*r* indices and found to show highest β_{total} value. If we compare these two series, it is exhibited that for both series thienothiophene π-conjugated linkers show highest Δ*r* indices and imidazolium acceptor system proves better for charge transfer. This can be well correlated with the 1st hyperpolarizability of the molecules. The integral overlap of hole electron distribution (*s*) is a tool to measure the spatial separation of hole and electron and the distance between the centroids of hole and electron (*D*), define the charge transfer length. Higher the value of *D*, more will be the charge transfer length. For CT transition mode, *D* should be large and *s* should be small. Smallest *s* value of 0.015 and highest *D* value of 21.04 Å are found for dye 2d which helps to understand the genesis of highest NLO response. The transition dipole moment densities are plotted in Fig. 5.5

Table 5.3. Major transition energy, Δ*r* index, integral overlap of hole electron distribution (*s*) and distance between centroid of hole and electron (*D*) calculated at CAM-B3LYP/6-311++G(d,p) level of theory.

Compound	State	Transition energy (eV)	Δ*r* (Å)	*s*	*D* (Å)
1	S5	2.915	12.332	0.042	11.33
1a	S3	2.714	12.261	0.162	7.51
1b	S5	2.566	14.107	0.146	9.63
1c	S5	2.742	17.394	0.136	16.29
1d	S5	2.436	17.801	0.135	13.47
2	S3	2.449	12.117	0.024	10.73
2a	S4	2.129	15.228	0.018	13.89
2b	S4	1.953	17.563	0.017	16.42
2c	S4	1.889	17.846	0.017	16.76
2d	S4	1.734	21.805	0.015	21.04

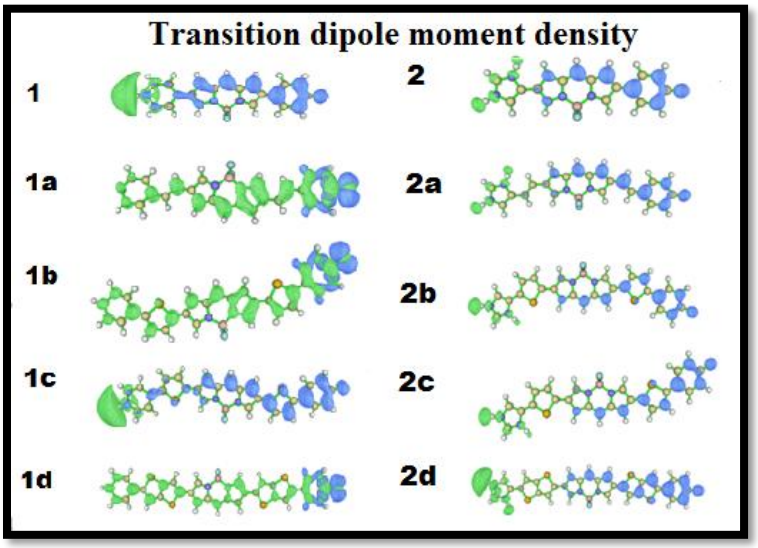

Fig. 5.5. The transition dipole moment density of the studied molecules (1 to 2d). Isovalue is 2×10^{-4}. The green colour implies charge increase upon excitation and the blue colour implies charge depletion.

5.3.3. UV-VIS spectra of dyes

Time dependent density functional theory (TDDFT) is used to calculate vertical excitation energy of the designed dyes. TDDFT computations are carried out using B3LYP and CAMB3LYP functionals with 6-311++G(d,p) basis set. TDDFT method is very popular choice for the calculation of vertical excitation energy. But there are some limitations while predicting the transition energy for charge transfer based molecules.[57] Jacquemin and co-workers performed computational analysis of the spectral properties of BODIPY derived systems with different functionals using TDDFT methodology[58] and compared results with experimental data. In this paper they also designed new aza-BODIPY molecules for near-infra red (NIR) application with the same methodology. So, here we take TDDFT to calculate absorption spectra of the designed dyes absorbing light in the NIR region. Long range correlated functional like CAM-B3LYP is better choice to calculate the vertical excitation energy to understand the charge transfer characteristics in molecules.[59, 60] Benchmarking of the TDDFT methodology has been done with some common BODIPY systems which are represented in Table 5.4.[25] The correlation of computed and experimental results induced us to choose CAM-B3LYP functional for the estimation of vertical excitation energy of our designed systems. The vertical excitation energy, maximum absorption wave length, oscillator strength and nature of transitions have been reported in Table 5.5 and Table S11 (Electronic supplementary information). When we compare Fig. 5.2, Table 5.5 and Table S11, we can found that the excitation energies in case of CAM-B3LYP functional are in consonance with the HOMO-LUMO gap of the molecules. In the following discussions results are illustrated by taking CAM-B3LYP functional. In all cases $S_0 \rightarrow S_1$ electronic transitions are dominated with high oscillator strength and for dyes 1b, 1c and 1d $S_0 \rightarrow S_2$ electronic transitions found with moderate oscillator strength. The excitation energies of dye 1 and dye 2 are 1.173 eV and 1.327 eV respectively. From these results, it has been found that substitutions of pyridinium acceptor by imidazolium acceptor in the BODIPY system, the absorption wavelength are blue shifted due to its high HOMO-LUMO gap compared to pyridinium acceptor. Table 5.5 indicates that when ethylene group is included in the D-π-A system in dye 1 and 2, the absorption maxima are red shifted by 29 nm and 88 nm respectively. This is due to the increases of π-conjugation length of the system. The excitation energy

systematically decreases with addition of thiophene π-linkers. Compared to cis-thiophene, trans-thiophene systems (1c and 2c) are red shifted by 128 nm and 143 nm. Maximum absorption wavelength found for dye 1d (1650 nm) and 2d (1471 nm) when thienothiophene groups are added as 1st and 3rd π-linker in BODIPY donor-acceptor system. The structural modification in the BODIPY system pushes the chromophore to absorb light in the NIR region (933 nm – 1471 nm). In both series the absorption wavelength are red shifted with the addition of π-linkers in the parent compounds. The increasing order of λ_{max} is as follows: 1< 1a <1b < 1c < 1d and 2 < 2a < 2b < 2c < 2d. Highest oscillator strength found for dye 1d which is 1.4957. Overall, it can be concluded that with the addition of different π-linkers in D-π-A system, λ_{max}, oscillator strength, ICT character can be systematically modified.

Table 5.4. TDDFT benchmarking of theoretical and experimental maximum absorption wavelength (λ_{max}), *f* represents oscillator strength.

Molecule	Solvent	Experiment λ_{max} (nm)	Theoretical λ_{max} (nm) 6-311++G(d, p)	
			B3LYP	CAM-B3LYP
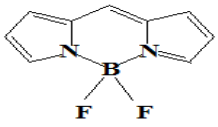	Methanol	497	415.4 *f* = 0.5047	418.1 *f* = 0.5979
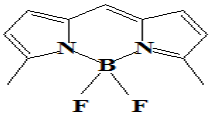	Ethanol	507	431.3 *f* = 0.5986	435.6 *f* = 0.6579
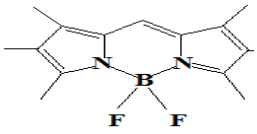	Ethanol	528	446.15 *f* = 0.5978	445.65 *f* = 0.7163

Table 5.5. Main electronic transitions, maximum absorption wavelength (λ_{max}), oscillator strength (***f***) and transition nature of BODIPY based dyes in gas phase at CAM-B3LYP/6-311++G(d,p) level of theory.

Dye	Excited energy (eV)	λ_{max} (nm)	*f*	Assignment	
1	1.173	1056.93	0.7333	H → L	0.667
1a	1.142	1085.95	1.3417	H → L	0.706
1b	0.932	1329.79	1.3891	H → L	0.737
	1.281	968.15	0.2467	H → L +1	0.689
1c	0.819	1512.20	1.4008	H → L	0.712
	1.218	1017.71	0.6243	H → L +1	0.657
1d	0.751	1649.98	1.4957	H → L	0.759
	1.128	1099.48	0.5036	H → L +1	0.683
2	1.327	933.96	0.4988	H → L	0.651
2a	1.214	1021.53	0.9052	H → L	0.539
2b	1.075	1153.25	1.1855	H → L	0.680
2c	0.957	1296.38	1.0327	H → L	0.655
2d	0.843	1471.35	1.052	H → L	0.775

5.3.4. Ionization potential, electron affinity and reorganization energy

Isolated molecule with low reorganization energy is associated with the high solid state charge carrier mobility.[61, 62] It is also found that some N-containing conjugated organic compounds found to be promising n-type or p-type materials for the fabrication of optical light emitting diode (OLED).[63, 64] This is arises due to their excellent optoelectronic properties, thermal stabilities and high electron mobilities etc. As hyperpolarizability is associated with the charge transfer from donor group to acceptor group, so determination of Ionization Potential (IP), Electron Affinity (EA) and

reorganization energy of organic molecules confer relevant information about the charge transport property and charge injection character of a molecule. Adiabatic IP, EA and reorganization energy of these ten molecules are calculated at B3LYP/6-311++G(d,p) level and represented in Table 5.6. For all the molecules, the potential energy of the cationic state are higher than the potential energy of the neutral state, this provides a positive ionization potential. In case of anion, potential energy is lower than the potential energy of the neutral state, which gives a negative EA. The IP and EA of studied dyes are in the range of 5.37 eV to 4.47 eV and 2.04 eV to 3.05 eV respectively. It is known that molecule with higher EA value shows higher electron transport ability and molecule with lower IP value shows higher hole transport ability.[65] Compound 2d has lowest IP value of 4.47 eV and 1d has highest EA value of 3.05 eV. So 1d and 2d molecules will transport electron and hole better than the other molecules. It is interesting to note that with the decrease of HOMO-LUMO gap in both systems IP values gradually decreases and EA values increase.

Table 5.6. Calculated ionization potentials (IP), electron affinities (EA), reorganization energies (λ_{hole} and $\lambda_{electron}$) of the dyes in gas phase at the B3LYP/6-311++G(d,p) level of theory (in eV).

Molecule	IP	EA	λ_{hole}	$\lambda_{electron}$
1	5.37	2.45	0.39	1.35
1a	5.20	2.67	0.12	0.19
1b	5.01	2.88	0.09	0.20
1c	4.96	2.90	0.09	0.19
1d	4.85	3.05	0.08	0.17
2	5.13	2.04	0.14	1.12
2a	4.83	2.11	0.13	0.27
2b	4.65	2.34	0.17	0.18
2c	4.59	2.37	0.11	0.23
2d	4.47	2.81	0.06	0.21

To examine the effect of various substitution on the reorganization energy for hole/electron transport ($\lambda_{hole\ /electron}$), λ_{hole} and $\lambda_{electron}$ are tabulated in Table 5.6. To obtain high efficiency optical light-emitting diode, it is exigent to optimize the charge carrier (electron/hole) injection process and electron-hole recombination process.[66] Also the charge injection and charge transport are crucial to ascertain the luminescence efficiency of OLED and it can be attained using separate electron transport material and hole transport material.[67] According to the Marcus theory reorganization energy is the deciding factor for the rate of charge transfer and this energy is required for structural changes associated with the charge transfer process.[68] It is well known that smaller the hole transport reorganization energy (λ_{hole}) better the hole transport property and smaller the electron transport reorganization energy ($\lambda_{electron}$) better the electron transport property. As expected with the increase of π-conjugation length λ_{hole} and $\lambda_{electron}$ values decreases for most of the cases. This implies that the hole/electron transport property increases along the series. The smallest λ_{hole} and $\lambda_{electron}$ found for thioenothiophene substituted linker in both the series which is in accordance with the NLO property of the molecule. This can be explained by the increase of rigidity and planarity of the molecule. Smallest λ_{hole} and $\lambda_{electron}$ found for dye 2d and dye 1d which can be correlated with the obtained IP and EA of the studied molecules. Most interestingly it is found that for all the cases λ_{hole} is smaller than $\lambda_{electron}$ which indicate that molecules are better hole transporters than electron transporters. The difference between λ_{hole} and $\lambda_{electron}$ of the compounds with π-spacers are less than 0.15 eV suggests that they can act as emitter with moderately high light–emitting efficiencies.[69] Thus the studied molecules are promising candidates as hole transport materials.

5.4. Conclusions

In the present computational study, two series of novel zwitterionic BODIPY based molecules with pyridinium and imidazolium electron acceptors, phenoxide unit as electron donor and various π-linkers are designed and their nonlinear optical properties are investigated. DFT based methods are employed to explore their electronic structure, dipole moment, polarizability, hyperpolarizability, absorption property, IP, EA and reorganization energy of these molecules. Our results reveal that with the introduction of

different π-linkers in the D-π-A systems, planarity is maintained and HOMO-LUMO gap is systematically decreased. It is observed that thienothiophene groups reduce ΔE more than the other π-linkers. This observation is also supported by the excitation energy calculated with the TDDFT approach. Small HOMO-LUMO gaps of the molecules prompt the systems to absorb light in the NIR region. The FMO analysis depicts that for Series 1 dyes, the electrons are delocalized throughout the molecules whereas for Series 2 dyes, the donor unit largely stabilizes the HOMO along with π-linker and LUMO is localized on the acceptor unit. The intramolecular charge transfer from phenoxide unit to imidazolium unit through the π-conjugated backbone plays a significant role to obtain large NLO response in Series 2 dyes. Computed β_{tot} values of the dyes are found to be 442 (for 1 dye) - 4110 (for 2d dye) times greater than the value of urea molecule. Among the studied molecules 2d exhibits highest β_{tot} value. Imidazolium acceptor shows better NLO response than pyridinium acceptor. It is also to be noted that dipole moment, polarizability and hyperpolarizability are consistent with the HOMO-LUMO gap of the molecules. Lowest electron transport reorganization energy (0.17eV) and highest EA found for dye 1d and smallest hole transport reorganization energy (0.06eV) and least IP found for dye 2d. Consequently 1d and 2d seems to be high efficient emitters with promising hole transport characteristics. Overall, all these investigated dyes show high NLO response. First hyperpolarizability of the molecules is found to respond dominantly in the z direction which indicates the course of charge transfer. A good correlation has been found between Δr index, TDM density, hyperpolarizability value and hole/electron transport property. As a whole, this work demonstrates that the structural modification of π-linkers and electron acceptors in designing D-π-A system is a significant approach to obtain of high performance NLO material.

5.5. References

1. Coe, B. J., *Coord. Chem. Rev.*, **2013**, 257, 1438-1458.
2. Marks, T. J.; Ratner, M. A., *Angew. Chem. Int. Ed. Engl.*, **1995**, 34, 155-173.
3. Lacroix, P. G., *Euro. J. Inorg. Chem.*, 2001, **2001**, 339-348.
4. Peng, Z.; Yu, L., *Macromolecules*, **1994**, 27, 2638-2640.
5. Tsutsumi, N.; Morishima, M.; Sakai, W., *Macromolecules*, **1998**, 31, 7764-7769.

6. Breitung, E. M.; Shu, C.-F.; McMahon, R. J., *J. Am. Chem. Soc.*, **2000**, 122, 1154-1160.
7. Dalton, L. R.; Sullivan, P. A.; Bale, D. H., *Chem. Rev.*, **2009**, 110, 25-55.
8. Di Bella, S., *Chem. Soc. Rev.*, **2001**, 30, 355-366.
9. Majumder, M.; Goswami, T.; Misra, A., *ChemistrySelect*, **2018**, 3, 933-939.
10. Roundhill, D. M.; Fackler Jr, J. P., *Optoelectronic properties of Inorg. Compd.*, Springer Science & Business Media, **2013**.
11. Sutradhar, T.; Misra, A., *ChemistrySelect*, **2019**, 4, 3697-3705.
12. Majumder, M.; Misra, A., *Phys. Chem. Chem. Phys.*, **2018**, 20, 19007-19016.
13. Kölmel, D. K.; Hörner, A.; Castañeda, J. A.; Ferencz, J. A.; Bihlmeier, A.; Nieger, M.; Bräse, S.; Padilha, L. A., *J. Phys. Chem. C*, **2016**, 120, 4538-4545.
14. Zyss, J., *Molecular nonlinear optics: materials, physics, and devices*, Academic press, **2013**.
15. Sharipova, S. M.; Kalinin, *Chem. Heterocyclic Comp.*, **2017**, 53, 36-38.
16. Teran, N. B.; He, G. S.; Baev, A.; Shi, Y.; Swihart, M. T.; Prasad, P. N.; Marks, T. J.; Reynolds, J. R., *J. Am. Chem. Soc.*, **2016**, 138, 6975-6984.
17. Yang, M.; Jacquemin, D.; Champagne, B., *Phys. Chem. Chem. Phys.*, **2002**, 4, 5566-5571.
18. Khan, M. U.; Khalid, M.; Ibrahim, M.; Braga, A. A. C.; Safdar, M.; Al-Saadi, A. A.; Janjua, M. R. S. A., *J. Phys. Chem. C*, **2018**, 122, 4009-4018.
19. Driessen, A., *Nonlinear Optics for the Information Society*, Springer, **2007**.
20. Janjua, M. R. S. A.; Khan, M. U.; Bashir, B.; Iqbal, M. A.; Song, Y.; Naqvi, S. A. R.; Khan, Z. A., *Comput. Theor. Chem.*, **2012**, 994, 34-40.
21. Albert, I. D.; Marks, T. J.; Ratner, M. A., *J. Am. Chem. Soc.*, **1997**, 119, 3155-3156.
22. Albert, I. D.; Marks, T. J.; Ratner, M. A., *J. Am. Chem. Soc.*, **1998**, 120, 11174-11181.
23. Geskin, V. M.; Lambert, C.; Brédas, J.-L., *J. Am. Chem. Soc.*, **2003**, 125, 15651-15658.
24. Xiong, Y.; Tang, H.; Zhang, J.; Wang, Z. Y.; Campo, J.; Wenseleers, W.; Goovaerts, E., *Chem. Mater.*, **2008**, 20, 7465-7473.
25. Loudet, A.; Burgess, K., *Chem. Rev.*, **2007**, 107, 4891-4932.
26. Sutradhar, T.; Misra, A. , *J.Phys. Chem. A*, **2018**, 122, 4111-4120.
27. Zhang, X.; Xiao, Y.; Qi, J.; Qu, J.; Kim, B.; Yue, X.; Belfield, K. D., *J. Org. Chem.*, **2013**, 78, 9153-9160.
28. Kamkaew, A.; Lim, S. H.; Lee, H. B.; Kiew, L. V.; Chung, L. Y.; Burgess, K., *Chem. Soc. Rev.*, **2013**, 42, 77-88.
29. Gabe, Y.; Urano, Y.; Kikuchi, K.; Kojima, H.; Nagano, T., *J. Am. Chem. Soc.*, **2004**, 126, 3357-3367.
30. Karolin, J.; Johansson, L. B.-A.; Strandberg, L.; Ny, T., *J. Am. Chem. Soc.*, **1994**, 116, 7801-7806.
31. Paul, A.; Mandal, P. K.; Samanta, A., *J. Phys. Chem. B*, **2005**, 109, 9148-9153.
32. Boydston, A. J.; Pecinovsky, C. S.; Chao, S. T.; Bielawski, C. W., *J. Am. Chem. Soc.*, **2007**, 129, 14550-14551.
33. Fuller, J.; Carlin, R.; Simpson, L.; Furtak, T., *Chem. Mater.*, **1995**, 7, 909-919.

34. Fortuna, C. G.; Bonaccorso, C.; Qamar, F.; Anu, A.; Ledoux, I.; Musumarra, G., *Org. & Biomol. Chem.*, **2011**, 9, 1608-1613.
35. Thakare, S. S.; Chakraborty, G.; Krishnakumar, P.; Ray, A. K.; Maity, D. K.; Pal, H.; Sekar, N., *J. Phys. Chem. B*, **2016**, 120, 11266-11278.
36. Prakasam, M.; Anbarasan, P. M., *RSC Advances.*, **2016**, 6, 75242-75250.
37. Avramopoulos, A.; Zaleśny, R.; Reis, H.; Papadopoulos, M. G., *J. Phys. Chem. C*, **2020**, 124, 4221-4241.
38. Yanai, T.; Tew, D. P.; Handy, N. C., *Chem. Phys. Lett.*, **2004**, 393, 51-57.
39. Frisch, M.; Trucks, G.; Schlegel, H.; Scuseria, G.; Robb, M.; Cheeseman, J., Gaussian 09, Revision B. 01, Gaussian Inc., Wallingford CT, **2009**.
40. Karakas, A.; Elmali, A.; Unver, H., *Spectrochimica Acta Part A: Mol. Biomol. Spectros.*, **2007**, 68, 567-572.
41. Lu, T., *Software manual. Version*, **2014**, 3.
42. Guido, C. A.; Cortona, P.; Mennucci, B.; Adamo, C., *J. Chem. Theo. Comp.*, **2013**, 9, 3118-3126.
43. Curioni, A.; Boero, M.; Andreoni, W., *Chem. Phys. Lett.*, **1998**, 294, 263-271.
44. Hutchison, G. R.; Ratner, M. A.; Marks, T. J., *J. Am. Chem. Soc.*, **2005**, 127, 2339-2350.
45. Kutzelnigg, W., *Angewandte Chemie*, **1992**, 104, 1423-1423.
46. Hu, R.; Lager, E.; Aguilar-Aguilar, A.; Liu, J.; Lam, J. W.; Sung, H. H.; Williams, I. D.; Zhong, Y.; Wong, K. S.; Pena-Cabrera, E., *J. Phys. Chem. C*, **2009**, 113, 15845-15853.
47. Chattaraj, P. K.; Sarkar, U.; Roy, D. R., *Chem. Rev.*, **2006**, 106, 2065-2091.
48. Gunasekaran, S.; Balaji, R. A.; Kumeresan, S.; Anand, G.; Srinivasan, S., *Can. J. Anal. Sci. Spectrosc.*, **2008**, 53, 149-162.
49. Khalid, M.; Ali, M.; Aslam, M.; Sumrra, S. H.; Khan, M. U.; Raza, N.; Kumar, N.; Imran, M., *Int. J. Pharm. Sci. Res.*, **2017**, 8, 457.
50. Zhang, H.; Yang, Y.; Xiao, H.; Liu, F.; Huo, F.; Chen, L.; Chen, Z.; Bo, S.; Qiu, L.; Zhen, Z., *J. Mater. Chem.C*, **2017**, 5, 6704-6712.
51. Oudar, J. d., *J. Chem. Phys.*, **1977**, 67, 446-457.
52. Verbiest, T.; Houbrechts, S.; Kauranen, M.; Clays, K.; Persoons, A., *J. Mater. Chem.*,**1997**, **7**, 2175-2189.
53. Zhang, T.; Yan, L.-K.; Cong, S.; Guan, W.; Su, Z.-M., *Inorg. Chem. Front.*, **2014**, 1, 65-70.
54. Paul, S.; Misra, A., *Inorg. Chem.*, **2011**, 50, 3234-3246.
55. Yu, H.-L.; Wang, W.-Y.; Hong, B.; Zong, Y.; Si, Y.-L.; Hu, Z.-Q., *Phys. Chem. Chem. Phys.*, **2016**, 18, 26487-26494.
56. Patil, P. S.; Maidur, S. R.; Shkir, M.; AlFaify, S.; Ganesh, V.; Krishnakanth, K. N.; Rao, S. V., *J. Appl. Crystallogr.*, **2018**, 51.
57. Dreuw, A.; Weisman, J. L.; Head-Gordon, M., *J. Chem. Phys.*,**2003**, 119, 2943-2946.
58. Le Guennic, B.; Maury, O.; Jacquemin, D., *PCCP*, **2012**, 14, 157-164.
59. Cai, Z.-L.; Crossley, M. J.; Reimers, J. R.; Kobayashi, R.; Amos, R. D., *J. Phys. Chem. B*, **2006**, 110, 15624-15632.
60. Kobayashi, R.; Amos, R. D., *Chem. Phys. Lett.*, **2006**, 420, 106-109.
61. Cheung, D. L.; Troisi, A., *Phys. Chem. Chem. Phys.*, **2008**, 10, 5941-5952.

62. Sakanoue, K.; Motoda, M.; Sugimoto, M.; Sakaki, S., *J. Phys. Chem. A*, **1999**, 103, 5551-5556.
63. Kim, J. Y.; Yasuda, T.; Yang, Y. S.; Adachi, C., *Adv. Mater.*, **2013**, 25, 2666-2671.
64. Zhao, C.; Ge, H.; Yin, S.; Wang, W., *J. Mol. Model.*, **2014**, 20, 2158.
65. Geng, Y.; Li, H.-B.; Wu, S.-X.; Su, Z.-M., *J. Mater. Chem.*, **2012**, 22, 20840-20851.
66. Jou, J.-H.; Kumar, S.; Agrawal, A.; Li, T.-H.; Sahoo, S., *J. Mater. Chem. C*, **2015**, 3, 2974-3002.
67. Peumans, P.; Yakimov, A.; Forrest, S. R., *J. Appl. Phy.*, **2003**, 93, 3693-3723.
68. Marcus, R. A., *Angew. Chem. Int. in Eng.*, **1993**, 32, 1111-1121.
69. Zou, L.-Y.; Zhang, Z.-L.; Ren, A.-M.; Ran, X.-Q.; Feng, J.-K., Feng, *Theor. Chem.*, **2010,** 126, (5-6), 361-369.